

Photo-renewable electroanalytical sensor for neurotransmitters detection in body fluid mimics

Valentina Pifferi^{1,2} · Guido Soliveri^{1,2} · Guido Panzarasa³ · Giuseppe Cappelletti^{1,2} · Daniela Meroni^{1,2} · Luigi Falciola^{1,2}

Received: 3 February 2016 / Revised: 21 March 2016 / Accepted: 1 April 2016 / Published online: 13 April 2016
© Springer-Verlag Berlin Heidelberg 2016

Abstract A composite electrode with a sandwich structure combining the properties of silver nanoparticles and a titania photoactive layer was used for the electroanalytical detection, by differential pulse voltammetry, of three neurotransmitters: dopamine, norepinephrine, and serotonin. The three analytes were determined at low detection limits (around 0.03 μM) also in the presence of conventional interferents, such as uric and ascorbic acids. The fouling of the electrode surface was overcome by irradiating the device with UVA light, restoring the initial sensor sensitivity. Dopamine, norepinephrine, and serotonin were determined also in simulated biological matrices: liquor (artificially reproduced cerebrospinal fluid) and serum. Moreover, the contemporaneous detection of dopamine and norepinephrine in simulated human urine solutions was also demonstrated, representing the first step towards clinical applications of the proposed methodology.

Keywords Self-cleaning electrode · Photo-renewable sensor · Composite electrode device · Neurotransmitters detection · Silver nanoparticles · Titanium dioxide

Introduction

The quantitative detection of analytes under physiological conditions is of critical importance in clinical diagnosis [1–3]. This is especially true for neurotransmitters (e.g., dopamine, norepinephrine, serotonin) because of their key role in behavior expression, during excessive oxidative stress events, for the early diagnosis of neurodegenerative diseases (such as Parkinson disease) [4, 5] and some kinds of tumors (e.g., pheochromocytoma) [6].

The most used analytical methods in clinical realities are based on chromatography, which often requires time-consuming pretreatments, long time of analysis, and high costs, although allowing the contemporaneous detection of the three aforementioned analytes. For these reasons, many studies could be found in the literature proposing robust alternatives, also for pre-screening applications [7].

In this context, the electroanalytical techniques seem to be promising since they display simplicity of use and maintenance, high efficiency, and accuracy, together with low costs [7]. Moreover, neurotransmitters are well suited for electroanalytical detection because their reaction potentials lie in the potential windows of carbon [8–12] and metal electrodes in physiological buffers. However, an efficient electroanalysis of such molecules has always been a challenge [13, 14] because of both selectivity [15, 16] and fouling [17–19] problems. Firstly, these analytes show similar electron oxidation reactions with similar peak potentials at physiological pH (around 7.4), making their discrimination tough. Secondly, these compounds undergo secondary reactions after the initial

Published in the topical collection *Chemical Sensing Systems* with guest editors Maria Careri, Marco Giannetto, and Renato Seeber.

Electronic supplementary material The online version of this article (doi:10.1007/s00216-016-9539-3) contains supplementary material, which is available to authorized users.

✉ Valentina Pifferi
valentina.pifferi@unimi.it

¹ Dipartimento di Chimica, Università degli Studi di Milano, Via Golgi 19, 20133 Milan, Italy

² Consorzio Interuniversitario Nazionale per la Scienza e Tecnologia dei Materiali, (INSTM), Via Giusti 9, 50121 Florence, Italy

³ Dipartimento di Scienze e Innovazione Tecnologica, Università del Piemonte Orientale “Amedeo Avogadro”, Viale T. Michel 11, 15100 Alessandria, Italy

electron transfer, often generating insulating polymeric products yielding rapid inactivation of the electrode surface. Thirdly, the problem of the interferents is severe: not only uric and ascorbic acids are always present together with neurotransmitters in biological fluids at a concentration 100- to 1000-fold higher than that of the analytes (nanomolar range), but their oxidation peaks occur also at the same potential of the analytes, resulting in poor selectivity and reproducibility. The ability to selectively determine dopamine and the other neurotransmitters in the presence of such interferents would permit the development of chemical sensors for clinical, biomedical, and in vivo monitoring [1, 7].

Among different methodologies tested, an innovative approach to increase the affinity of the surface for the analyte and to lower the detection limits involves the use of highly engineered electrodes modified with nanomaterials (Ag, Au, Pt nanoparticles), polymer brushes, self-assembled monolayers, etc. [20]. However, fouling remains a big issue, especially if analysis was performed in biological matrices [19, 20]. In fact, electrode surface regeneration techniques such as mechanical cleaning (with grit paper, aggressive chemical etching) or electrochemical cleaning (e.g., for platinum or gold electrodes), despite being a common practice for bulk-metal electrodes [21] are not usable for these sophisticated sensors. In order to solve this problem, the use of cheap, single-use electrodes based on electrochemically treated pencil leads has been proposed [22]. These systems offer a good solution for fouling phenomena, but sensitivity and reproducibility worsen. A different approach involves the development of photo-renewable electrode surfaces which can easily regenerate themselves. In this context, we have recently reported an example of an electrochemical sensor that could be cleaned simply by UVA-light irradiation (thanks to its photo-active surface) and reused indefinitely [23], permitting its use also in on-field applications [24]. In this paper, we would like to show the potentialities of this device towards the contemporaneous detection of dopamine, norepinephrine, and serotonin in body fluid mimics.

Materials and methods

Materials

Dopamine, norepinephrine, and serotonin hydrochlorides were purchased from Sigma-Aldrich. Ascorbic and uric acids (Sigma-Aldrich) were used as interferents. Sodium chloride, sodium bicarbonate, sodium sulphate, potassium chloride, potassium phosphate dibasic trihydrate, magnesium chloride hexahydrate, calcium chloride, hydrochloric acid, tris(hydroxymethyl)aminomethane, glucose, disodium phosphate, and monosodium phosphate, purchased by Sigma-Aldrich (reagent grade purity), were used to prepare

the artificial liquor and serum (see [Electronic Supplementary Material](#), ESM). Bovine serum albumin (Sigma-Aldrich) was employed as mimic of serum proteins. All chemicals were used as received. Distilled water purified with a Millipore Milli-Q apparatus (resistivity $\geq 18.2 \text{ M}\Omega \text{ cm}^{-1}$) was used to prepare all solutions and sols.

Preparation of the device

Device assembly was accomplished according to a previously reported protocol [23]. The fluorine-doped tin oxide-coated glass slides (FTO, Sigma-Aldrich®, $\sim 7 (\Omega \text{ sq})$, $2 \times 3 \text{ cm}$) adopted as conductive supports were cleaned by sonication in a H_2O /acetone/propanol = 1:1:1 mixture and then irradiated for 1 h under UV light from a halogenide lamp (see below). The silica sol was prepared by the procedure previously reported by Wang et al. [25]. Briefly, 10 g of TEOS (Sigma-Aldrich) was added dropwise into a solution containing 225 g of ethanol and 4.5 g of hydrochloric acid (0.1 M). The mixture was stirred at room temperature for 2 h and then refluxed at 60 °C for 60 min. Eventually, 225 g of a CTAB (cationic surfactant, Sigma-Aldrich) solution in ethanol (2 g in 25 mL) was mixed with the as-obtained solution under gentle stirring at room temperature for 1 h. The FTO was dip-coated in the obtained sol and calcined at 500 °C for 1 h under N_2 flow. Before functionalization by (3-aminopropyl)triethoxysilane (APTES, Sigma-Aldrich), the silica layer was irradiated under UV for 1 h and dipped into anhydrous toluene under N_2 at 70 °C for 1 h. The functionalization was performed by immersing the substrate into a solution of 50 μL -APTES in 20 mL anhydrous toluene for 3 h at 70 °C. The sample was post-treated by sonication for few minutes in toluene, ethanol, and water to desorb the un-grafted siloxane molecules and eventually dried under a nitrogen stream. The sample was then immersed in a solution of Ag nanoparticles for 15 min to allow their attachment and dried under nitrogen flux. The top titania layer was obtained by dipping the sample in a titania sol and calcining it under N_2 flow for 1 h at 400 °C. The titania sol was developed in our group as previously reported [26, 27]. Briefly, 0.9 mL of HCl 37 % was added to a solution of $\text{Ti}(\text{OC}_3\text{H}_7)_4$ in ethanol (0.1 mol in 100 mL) under stirring. Then, 0.47 g of Lutensol ON70 (BASF) was added to the sol after being dissolved in 100 mL of ethanol. Silver nanoparticles (Ag NPs) were synthesized by adapting the procedure reported by Panzarasa [28]. Briefly, 0.15 g of silver nitrate was dissolved in 25 mL of water and this solution was added under stirring to a solution of 0.5 g of trisodium citrate and 0.25 g of poly(vinylpyrrolidone) (PVP10, $M_w \sim 10000 \text{ (g mol}^{-1}\text{)}$, Sigma-Aldrich) in 125 mL of water. The resulting solution was poured in a three-necked, round-bottomed 250-mL flask equipped with a mechanical stirrer and a dropping funnel. The solution was cooled in an ice bath and an ice-cooled solution of sodium borohydride, obtained

by dissolving 12 mg of solid in 30 mL of water, and was added dropwise under stirring. The resulting dark brown suspension was stirred for 5 min, then aged at +4 °C for 24 h before use, and stored at this temperature.

Electrochemical setup

The detection of neurotransmitters was performed in a conventional three electrodes electrochemical cell, using a saturated calomel, a Pt wire and the electrode device as reference, counter and working electrodes, respectively. Phosphate buffer (pH 7.4, 0.1 M) was used as supporting electrolyte for the optimization of the analytical method. Cyclic voltammetry (CV), electrochemical impedance spectroscopy (EIS), pulsed and linear voltammeteries, and chrono methods were carried out with an Autolab PGStat30 (Ecochemie, The Netherlands) potentiostat/galvanostat equipped with FRA module and controlled by NOVA and FRA softwares. Impedance data were processed with Z-View 3.1 software. No N₂ degassing of the solution was necessary since dissolved O₂ did not affect the measurements. All the linear and pulsed voltammeteries and the chronoamperometry were performed with the parameters reported in the discussion section. Electrochemical impedance spectra were registered at -0.1, +0.1, and +0.25 V (SCE) in a frequency range between 65000 and 0.1 Hz and an amplitude of 10 mV.

Self-cleaning procedure

The fouling of the electrode was verified by the presence of the neurotransmitter peak at 0.3 V and the decrease/disappearance of the silver peak at 0.17 V (Fig. 1a), registering voltammograms in the electrolyte solution. The regeneration of the electrode surface was performed by irradiating for 1 h under UV-A light. An UV iron halogenide lamp Jelosil HG500 with an effective power density of 23 mW cm⁻², measured using a Thorlabs S314C radiometer, and emitting between 280 and 400 nm was used for the electrode self-cleaning procedure. After the irradiation, the electrode cleaning was confirmed by registering a new voltammogram in the electrolyte solution, verifying the absence of the neurotransmitter peak and the restoration of silver peak (Fig. 1a, after UV).

Results and discussion

Structure and features of the device

The structure of the sensor was engineered to condense in a single device the more desirable features for efficient electroanalysis of neurotransmitters (Fig. 1b). The FTO-coated conductive glass supports a sol-gel deposited silica layer.

The SiO₂ surface (550 nm thick [23]) is functionalized with a self-assembled monolayer of an amine-terminated siloxane (3-aminopropyl triethoxysilane, APTES) acting as a columbic binder to anchor negatively charged AgNPs (~10 nm diameter) at the surface. The Ag NPs are the active core of the device, imparting their electrocatalytic properties [29–32]. As previously discussed [23], the role of silica layer is crucial since it governs the morphology and the number of active sites, leading to tailored distribution of the Ag nanoparticles at the surface. Briefly, the particles are arranged in a homogeneous and well-separated way, which maximizes faradaic currents with the minimum quantity of active metal through the onset of the convergent diffusion regime [33, 34] (see also ESM for major details); this effect is accompanied by the lowering of the capacitive currents [35–37]. Finally, AgNPs are completely embedded in a porous anatase titania layer (150 nm [23], Fig. 1c), which confers other fundamental features to the device: (i) it increases the selectivity through the electrostatic repulsion of negatively charged interferences, (ii) it prevents silver nanoparticles from oxidative deactivation, and (iii) it confers photoactivity that can be used for UVA-cleaning. Thanks to these features, the device is reusable for hundreds of times through a simple regeneration step (Fig. 1a), which is able to recover the original sensitivity, as previously demonstrated [23]. XPS analyses confirmed the complete restoration of the electrode surface after the cleaning process, as shown in the ESM (Fig. S1 and Table S1). This self-cleaning property is due to the top titania layer and performs efficiently not only against the fouling due to the neurotransmitters themselves, but also against the passivation caused by interferences and organic/inorganic molecules present in the complex biomatrices.

Electrochemical characterization

The best electroanalytical technique, among the several tested (linear and cyclic voltammeteries, square wave voltammetry, and chronoamperometry), in terms of detection limits and sensitivity, is differential pulse voltammetry (DPV), whose parameters (modulation and interval times) were optimized. The analysis was performed in 0.1 M phosphate buffer solution (pH = 7.4), routinely used to simulate the biological environment. Probably, the fast scan of the other tested methodologies and the fixed potential used in amperometry were more affected by electrode fouling than DPV, causing worst results.

Figure 2 shows differential pulse voltammograms of the three tested molecules (dopamine, norepinephrine, serotonin) comparing the device with and without Ag (device and control, respectively). In the case of dopamine (as previously demonstrated [23]), the peak displacement towards less positive potential (from +0.23 to +0.16 V) indicates the electrocatalytic role of silver. On the other hand, norepinephrine and

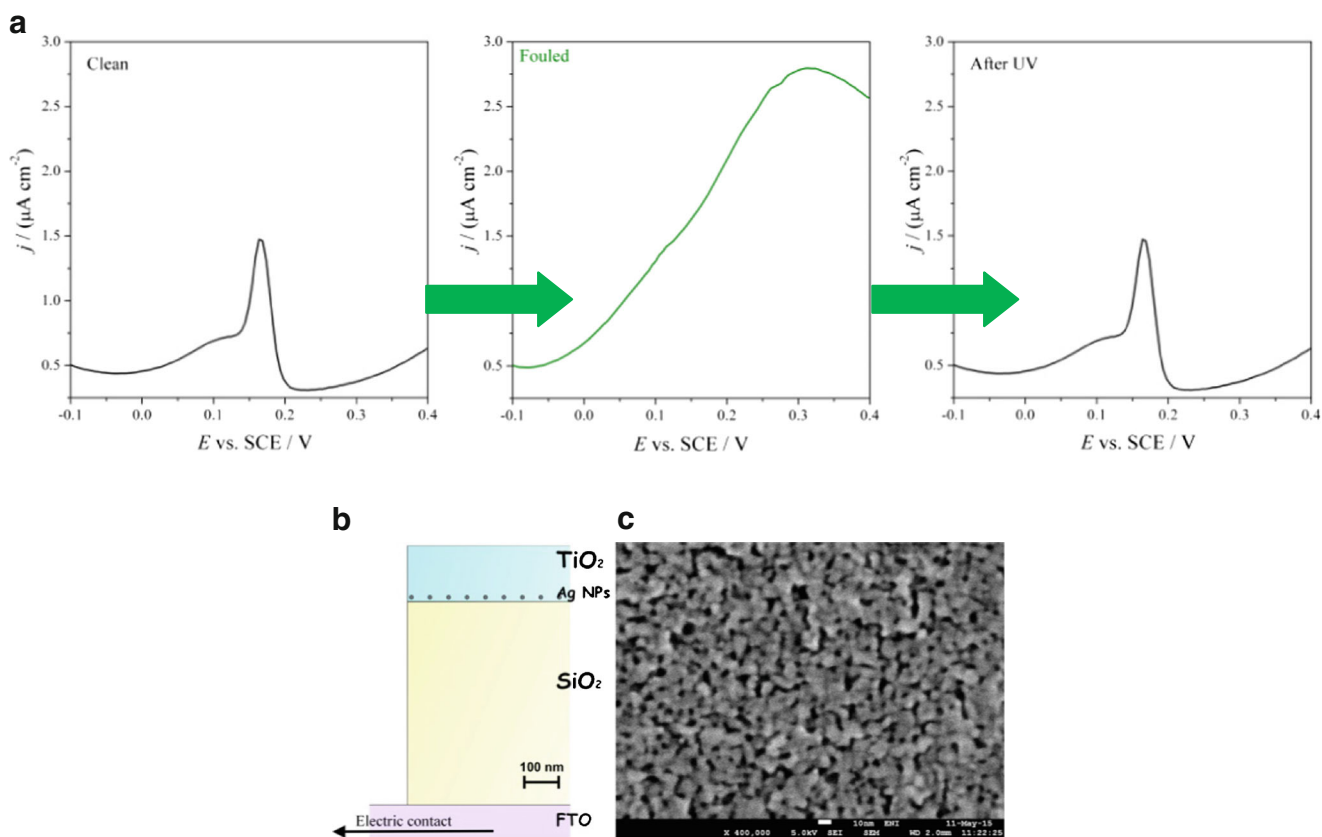


Fig. 1 a Differential pulse voltammograms showing the self-cleaning procedure steps, b schematic structure of the sensor device, c SEM image of the TiO₂ porous top layer

serotonin display on the electrode without silver a shoulder at +0.30 and +0.27 V, which increases with neurotransmitter concentration. The shoulder becomes a well-defined peak when AgNPs embedding devices are used, making the detection undoubtedly easier. The appearance of a better defined peak is probably due to the establishment of a convergent diffusion regime on a random assembly of silver nanoelectrodes, which is capable of increasing the peak currents, as explained in the ESM.

Figure 3 shows impedance complex plane spectra registered for the sensor with (device) and without (control) silver in the presence of the three molecules at the two different potentials: +0.25 and +0.1 V (SCE). Impedance complex plane spectra registered at -0.1 V (SCE) are also available in the ESM (Fig. S2).

The spectra display the typical trend for faradaic reactions, with a semicircle covering the entire frequencies range. The equivalent circuit (Fig. S3, ESM) used to fit all the samples

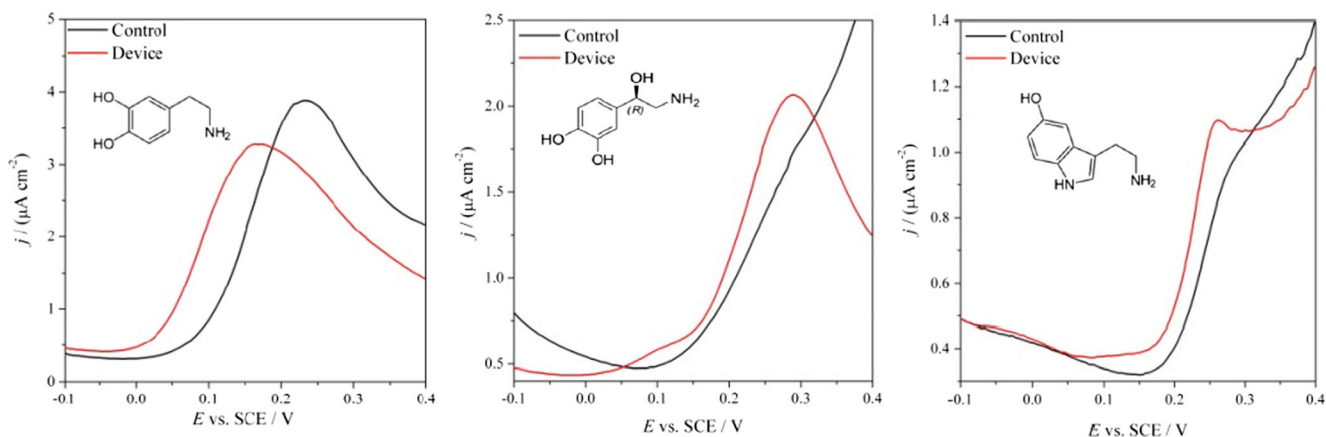


Fig. 2 Differential pulse voltammograms obtained in the presence of the three neurotransmitters (dopamine, norepinephrine, serotonin) at 0.1 mM concentration showing the differences obtained for the control (black lines, no silver) and the device (red lines, AgNPs) electrodes

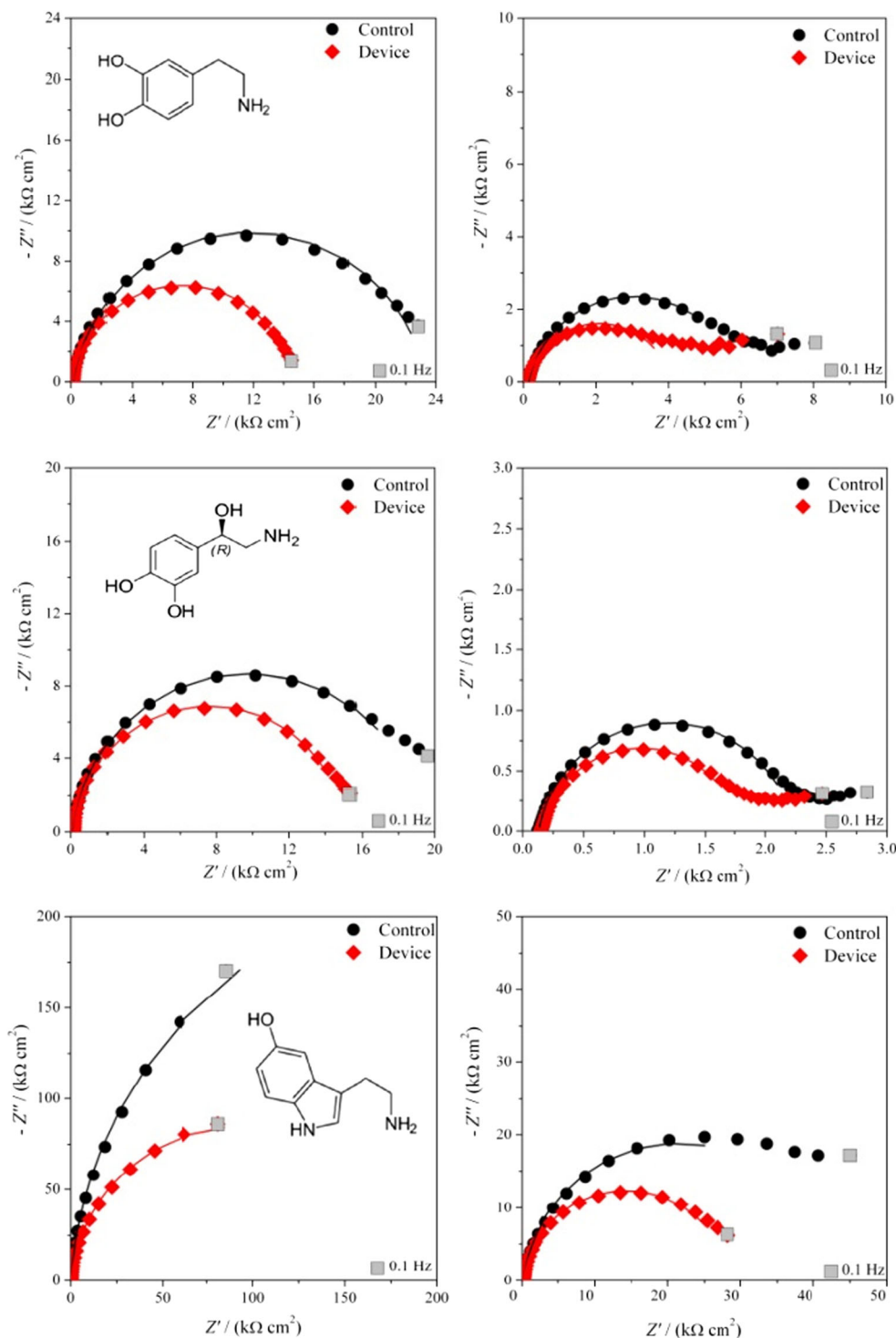


Fig. 3 Complex plane plots (from 65000 to 0.1 Hz) at +0.1 V (left) and +0.25 V (right) in the presence of dopamine, norepinephrine, or serotonin for the control and the device

data is composed by the resistance of solution R_{Ω} in series with the charge transfer resistance R_{ct} and double-layer capacitance in parallel. This last parameter was modeled as a constant phase element $CPE_{dl} = [(Ci\omega)^{\alpha}]^{-1}$, representing the

charge separation of the double layer, which behaves as pure capacitor in the case of $\alpha = 1$ or as non-ideal capacitor, due to the porosity and non-homogeneity of the surface, for $0.5 < \alpha < 1$. The samples here considered present values of α

Table 1 Values of charge transfer resistance obtained from impedance fitting

$R_{ct} / (k\Omega \text{ cm}^2)$	Dopamine		Norepinephrine		Serotonin	
	+0.1 V	+0.25 V	+0.1 V	+0.25 V	+0.1 V	+0.25 V
Control	23	6	19	2	461	42
Device	14	4	15	1	184	28

around 0.9 (Table S2, ESM), indicating quite homogeneous surfaces. Capacitance values and solution resistances (Table S2, Fig. S2 ESM) are very similar for all the samples.

Table 1 shows the charge transfer resistance values obtained from the fitting. Dopamine and norepinephrine present lower absolute impedance and charge transfer resistance values with respect to serotonin, indicating their easier reaction probably due to the intrinsic structure of these molecules. In particular, dopamine and norepinephrine present more affinity for the titania surface: other authors report the adsorption of catecholamines through a strong interaction between the titania surface layer and the two OH groups [38, 39]. No literature results are reported in the case of serotonin adsorption onto titania, but a study on silver reveals that, in this case, the molecule is flatly located on the surface [40]. The last adsorption configuration allows a less packed structure, confirming our results.

It is worthwhile noticing that the presence of silver nanoparticles in the device structure is crucial to allow an easier reaction characterized by lower R_{CT} and impedance values.

Electroanalytical characterization

The optimized device was tested for the electroanalytical detection of the three neurotransmitters by differential pulse voltammetry. Table 2 reports the analytical parameters obtained for consecutive additions of the analytes in the 0–5 μM range. The sensitivity S of the method was obtained from the slope of

the calibration plots and LoD (1) and LoQ (2) were calculated following the IUPAC protocol [41, 42]:

$$LoD = 3.29 \frac{\sigma_{\text{Blank}}}{S} \quad (1)$$

$$LoQ = 10 \frac{\sigma_{\text{Blank}}}{S} \quad (2)$$

Where σ_{Blank} is the blank standard deviation. Since no blank signal was detected, this parameter was identified as the standard deviation obtained from the calibration plot.

Uniformly distributed residuals and very good correlation coefficients testify the good linearity of the calibration plots. The presence of silver increases the sensitivity and decreases LoD and LoQ of one order of magnitude. The repeatability and thus the best achievable internal precision of the method was evaluated by measuring in a short interval of time the peak current of 10 repeated scans of the same sample solution at different concentrations. The relative standard deviation of these measurements (RSD%) for three different concentrations and for three different electrodes is reported in Table 3. The intermediate (run-to-run or extra-day) repeatability was demonstrated by evaluating the precision in different days for 1 month. Trueness was evaluated by spiking and recovery. The analyte addition methodology was used, where the pseudo-unknown sample at three different values of concentration (the 2nd, the 5th, and the 8th of the calibration plot) was spiked in the solution after consecutive additions of a standard. The % apparent recovery factors (ARF %) were calculated as the percentage relative error between the measured and the true values. The results (Table 2) are very close to 100 % in all cases.

Interferents study

Ascorbic and uric acids are reported to be the major interferents during neurotransmitters detection because they usually react at the same potential of the analytes. Moreover, they are present in the biological fluids in concentrations from

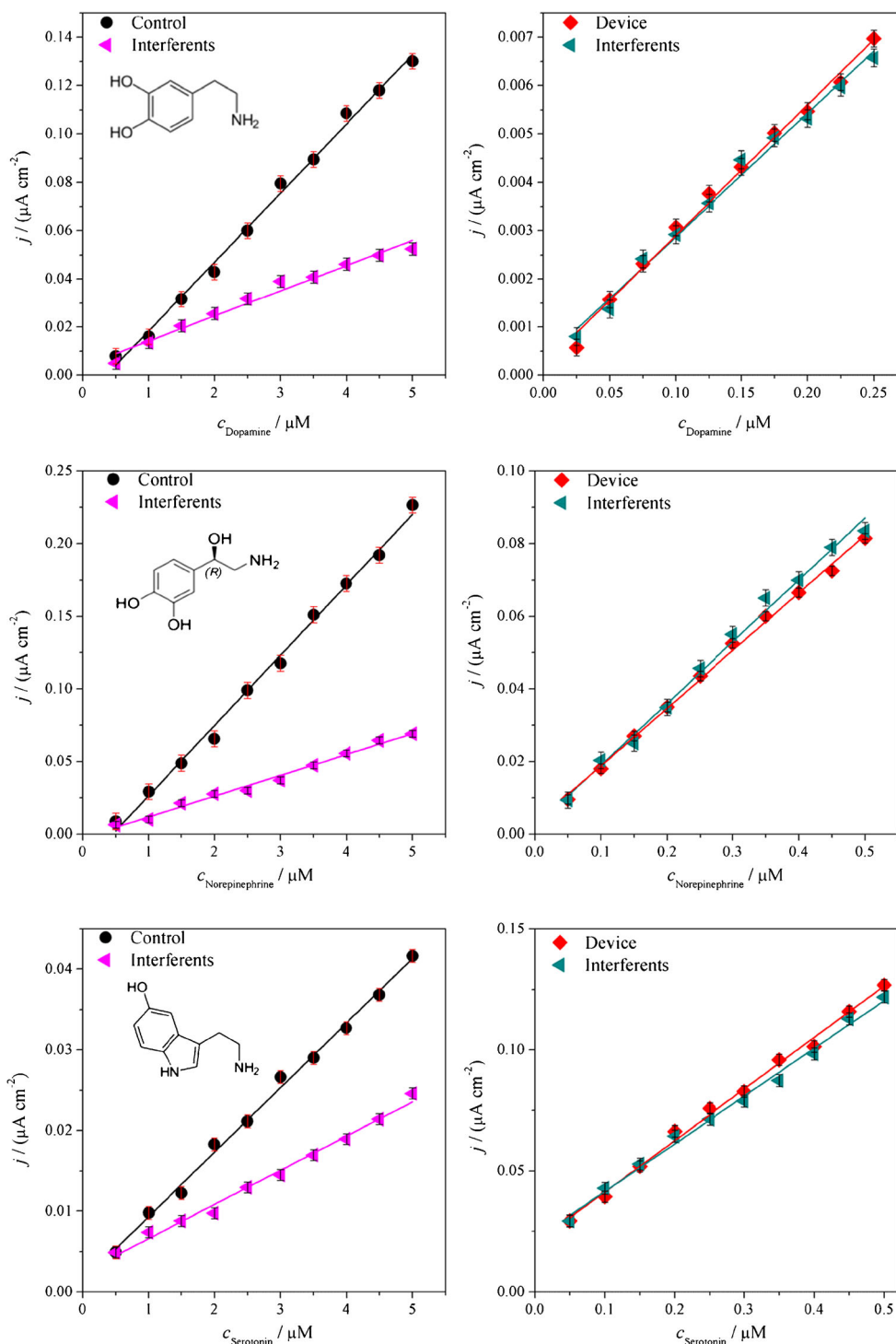
Table 2 Analytical parameters obtained for the control and the device during the detection of neurotransmitters

	Control			Device		
	Dopamine	Norepinephrine	Serotonin	Dopamine	Norepinephrine	Serotonin
$S / (\mu\text{A cm}^{-2} \mu\text{M}^{-1})$	0.0286 ± 0.0007	0.048 ± 0.001	0.008 ± 0.002	0.0256 ± 0.0008	0.159 ± 0.003	0.213 ± 0.005
LoD / μM	0.37	0.37	0.33	0.03	0.04	0.04
LoQ / μM	1.12	1.13	1.00	0.10	0.13	0.11
R^2	0.995	0.995	0.996	0.993	0.993	0.995
R^2_{adj}	0.994	0.994	0.995	0.993	0.992	0.995
RSD %	3	5	0.8	3	2	2
ARF %	104-100-98	104-100-98	104-100-98	101-99-99	101-99-99	101-99-99

Table 3 Sensitivities calculated from the slope of the calibration plots for the control and the device in the presence of the three neurotransmitters and ascorbic and uric acid as interferences

$S / (\mu\text{A cm}^{-2} \mu\text{M}^{-1})$	Dopamine		Norepinephrine		Serotonin	
	Alone	AA + UA	Alone	AA + UA	Alone	AA + UA
Control	0.0286	0.010	0.048	0.014	0.008	0.004
Device	0.0256	0.026	0.159	0.170	0.213	0.197

Fig. 4 Calibration plots obtained for the control (*left*) and the device (*right*) in the presence of the three neurotransmitters and ascorbic and uric acid as interferences



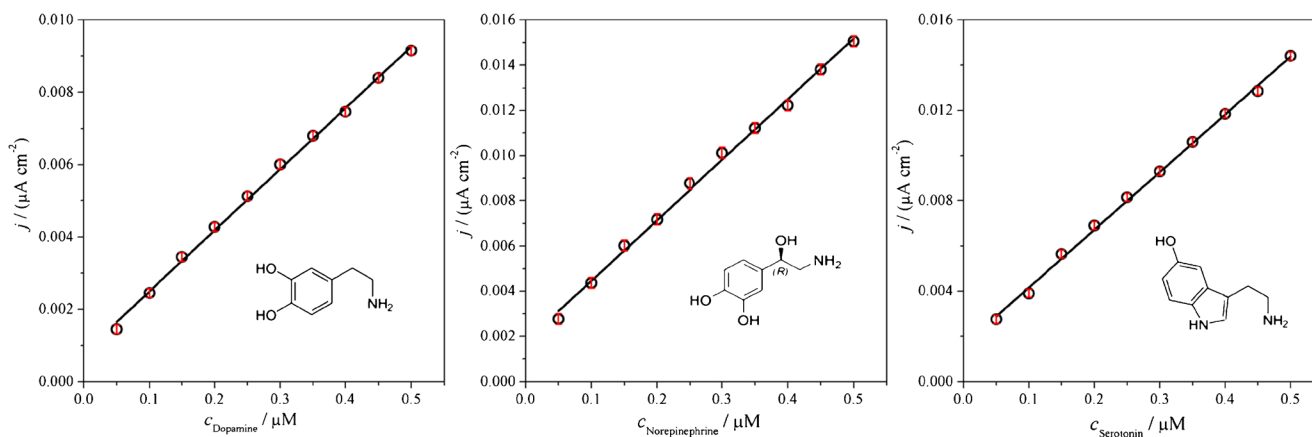


Fig. 5 Calibration plots obtained for the three neurotransmitters using liquor as biological matrix

100 to 1000 times higher than those of neurotransmitters, causing a critical matrix effect often very difficult to manage [7, 20]. Furthermore, especially in the case of ascorbic acid, the electrode surface can also be readily fouled by accumulation of its oxidation products [43].

In our case, the electroanalytical detection of the three neurotransmitters is possible (low or absent interferents' effect) also in the presence of high quantities of ascorbic and uric acids (0.1 mM for both acids) and calibration plots with good linearity could be obtained for both the device and the control (Fig. 4 and Table 3). One possible reason of this behavior could be found, considering that, at our working conditions (pH 7.4), the titania layer is negatively charged [44], thus acting as repelling barrier for negatively charged interferents (ascorbic acid $pK_{a1}=4.10$; uric acid $pK_{a1}=5.4$ [45]). On the other hand, the catecholamines are positively charged (dopamine $pK_{a1}=8.87$; norepinephrine $pK_{a1}=8.58$; serotonin $pK_{a1}=10.73$), and they are therefore electrostatically attracted by titania through the protonated primary amine group. A voltammetric experiment performed using a negatively charged redox probe $[\text{K}_4\text{Fe}(\text{CN})_6]$ confirmed this hypothesis.

As Fig. S4 demonstrates, the insertion of the titania layer completely abates the voltammetric peak of the probe, visible in the case of the FTO support.

In the case of the silver-containing device, not only the sensitivities are better (Table 3) and the analytical working range lower (Fig. 4), but the interferents do not affect the measurements at all and the sensitivities are completely maintained (Fig. 4), thus demonstrating once more the key role of convergent diffusion on Ag NPs.

Electroanalytical application in real matrices: liquor and serum

In order to test the efficiency of the sensor in real matrices, the detection in two biological fluids was investigated: artificially reproduced cerebrospinal fluid (liquor) and serum, both presenting high concentrations of interfering inorganic and organic substances. Artificial liquor (pH=7.5) and serum (pH=7.4) were prepared following protocols already described in the literature (Table S3, ESM) [46–51]. In these

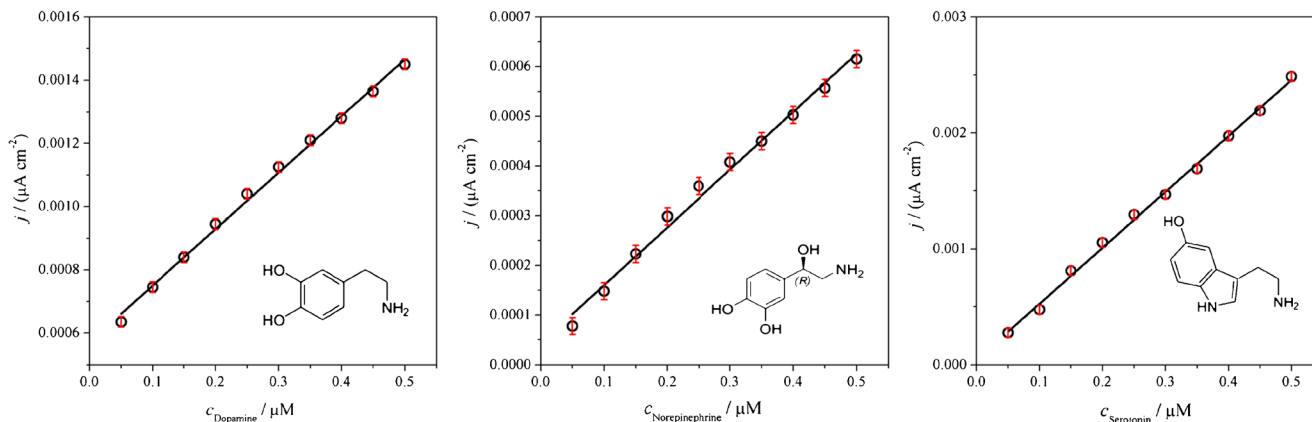
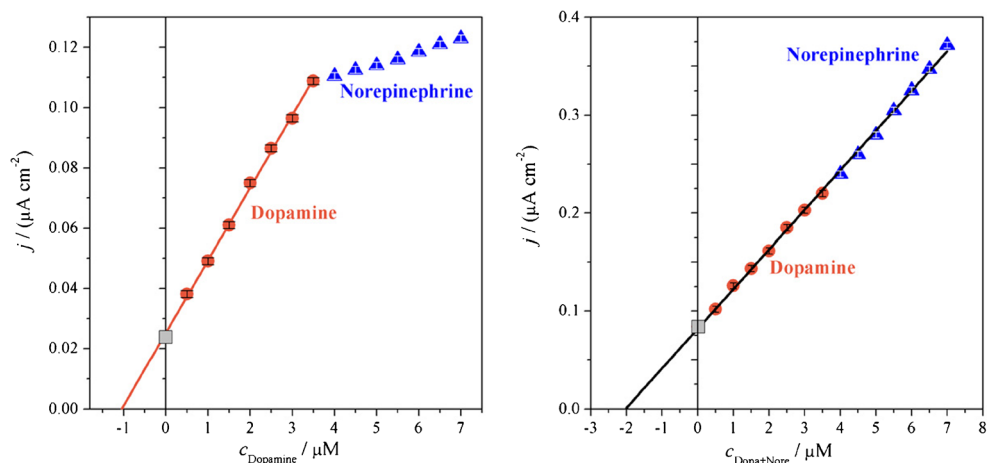


Fig. 6 Calibration plots obtained for the three neurotransmitters using serum as biological matrix

Fig. 7 Standard additions of dopamine and norepinephrine in a matrix spiked with 1.00 μM of both neurotransmitters. Determination of dopamine at 0.15 V (left) and of the sum of dopamine and norepinephrine at 0.3 V (right)



cases, the use of a supporting electrolyte was not necessary for electrochemical measurements.

Figures 5 and 6 show the calibration plots obtained for the three neurotransmitters detected in liquor and serum, respectively. The detection is characterized (Table 4) by good linearity ranges and good sensitivities (albeit lower, particularly for serum, with respect to the analysis in phosphate buffer). However, the limits of detection remain low, well below the requirements of the clinical application (0.1 μM).

Towards electroanalytical application in real matrices: the urine case

Among all the possible matrixes where neurotransmitters can be found, human urine (pH=6) represents one of the biggest challenge [7, 20]. In this matrix, where only dopamine and norepinephrine can be found, the determination is usually complicated because of the difficulty of the conventional electrodes to discriminate between the two neurotransmitters and the strong fouling. In this first attempt towards the contemporaneous determination of dopamine and norepinephrine, the two molecules were studied at concentrations in accordance with the levels normally detected in the urine biological matrix

Table 4 Analytical parameters obtained using liquor and serum as biological matrixes

	Liquor		
	Dopamine	Norepinephrine	Serotonin
$S/(\mu\text{A cm}^{-2}\mu\text{M}^{-1})$	0.0169	0.0268	0.0255
LoD / μM	0.02	0.03	0.02
	Serum		
	Dopamine	Norepinephrine	Serotonin
$S/(\mu\text{A cm}^{-2}\mu\text{M}^{-1})$	0.00179	0.00116	0.00483
LoD / μM	0.09	0.05	0.03

[49]. The analysis was performed by the standard addition technique exploiting dopamine and norepinephrine different peak potentials, which allow their discrimination.

Dopamine, in the presence of not interfering norepinephrine, was revealed at +0.15 V (Fig. 7a). At a higher potential value (+0.3 V), both molecules were detected (Fig. 7b) and the quantity of norepinephrine was calculated from the difference of the two values. As reported in Table 5, apparent recovery factors (ARF%) for the two molecules are good, showing the trueness of the method for their contemporaneous determination.

Conclusions

A new electroanalytical method was developed for the determination of dopamine, norepinephrine, and serotonin based on a sandwich structure sensor, ad hoc designed for this application. The electrode was composed by engineered silver nanoparticles, allowing a convergent diffusion regime, which was found to play a pivotal role in the recognition process. Such particles were covered by a photoactive titania layer that enabled the electrode regeneration under UV-A irradiation. Thanks to this configuration, the detection limits were found to be lower (0.03 μM) than the clinical requirement in routine analysis [7], also in the presence of typical interfering compounds, i.e., ascorbic and uric acids (1000:1). In biological matrixes, liquor, and serum, the situation was worsened by

Table 5 Apparent recovery factors obtained for the contemporaneous detection of two neurotransmitters

	Added / μM	Found / μM	ARF %
Dopamine	1.00	1.04	104
Norepinephrine	1.00	0.98	98

the presence of numerous charged compounds and proteins, which cause interference by reaction at the electrode or passivation of the active surface. However, also in this context, thanks to the great affinity with the analytes and its charge, TiO₂ demonstrated its key role repelling negatively charged interferents by electrostatic interactions and facilitating the detection with high selectivity. Moreover, its self-cleaning property was crucial to overcome the fouling phenomenon due to byproducts, collateral reactions of interferents, and passivation of the sensor. By simply irradiation with UV-A light, the electrode surface was completely regenerated and used for many further analyses.

Acknowledgments This work has been supported by Fondazione Cariplo (Italy), grant no. 2014-1285. The authors wish also to thank Dr. Laura Meda and Dr Gianluigi Marra from ENI Donegani Institute (Novara), for kindly providing SEM and XPS analyses.

Compliance with ethical standards

Conflict of interest The authors declare no conflict of interest.

References

- Robinson DL, Hermans A, Seipel AT, Wightman RM. Monitoring rapid chemical communication in the brain. *Chem Rev*. 2008;108:2554–84. doi:10.1021/cr068081q.
- Venton BJ, Wightman RM. Psychoanalytical electrochemistry: dopamine and behavior. *Anal Chem*. 2003;75:414A–21. doi:10.1021/ac031421c.
- Meiser J, Weindl D, Hiller K. Complexity of dopamine metabolism. *Cell Community Signal*. 2013;11:34. doi:10.1186/1478-811X-11-34.
- Segura-Aguilar J, Paris I, Muñoz P, Ferrari E, Zecca L, Zucca FA. Protective and toxic roles of dopamine in Parkinson's disease. *J Neurochem*. 2014;129:898–915. doi:10.1111/jnc.12686.
- Curulli A. Electrochemical direct determination of catecholamines for the early detection of neurodegenerative diseases. *Sensors*. 2009;9:2437–45. doi:10.3390/s90402437.
- Pacak K, Jacques WM, Lenders GE. Pheochromocytoma: diagnosis, localization, and treatment. Hoboken: Wiley; 2007.
- Perry M, Li Q, Kennedy RT. Review of recent advances in analytical techniques for the determination of neurotransmitters. *Anal Chim Acta*. 2009;653:1–22. doi:10.1016/j.aca.2009.08.038.
- Jemelková Z, Zima J, Barek J. Electroanalysis of some catecholamines at a single-wall nanotubes modified carbon paste electrode. *Collect Czechoslov Chem Commun*. 2010;75:1217–28. doi:10.1135/cccc2010076.
- Jemelkova Z, Barek J, Zima J. Determination of epinephrine at different types of carbon paste electrodes. *Anal Lett*. 2010;43:1367–76. doi:10.1080/00032710903518773.
- Hocevar SB, Wang J, Deo R, Musameh M, Ogorevc B. Carbon nanotube modified microelectrode for enhanced voltammetric detection of dopamine in the presence of ascorbate. *Electroanalysis*. 2005;17:417–22. doi:10.1002/elan.200403175.
- Lim CS, Chua CK, Pumera M. Detection of biomarkers with graphene nanoplatelets and nanoribbons. *Analyst*. 2014;139:1072–80. doi:10.1039/c3an01585h.
- Ghica ME, Brett CMA. Simple and efficient epinephrine sensor based on carbon nanotube modified carbon film electrodes. *Anal Lett*. 2013;46:1379–93. doi:10.1080/00032719.2012.762584.
- Lane RF, Hubbard AT. Differential double pulse voltammetry at chemically modified platinum electrodes for in vivo determination of catecholamines. *Anal Chem*. 1976;48:1287–92. doi:10.1021/ac50003a009.
- Henstridge MC, Dickinson E, Aslanoglu M, Batchelor-McAuley C, Compton RG. Voltammetric selectivity conferred by the modification of electrodes using conductive porous layers or films: the oxidation of dopamine on glassy carbon electrodes modified with multiwalled carbon nanotubes. *Sensors Actuators B Chem*. 2010;145:417–27. doi:10.1016/j.snb.2009.12.046.
- Oleinick A, Zhu F, Yan J, Mao B, Svir I, Amatore C. Theoretical investigation of generator-collector microwell arrays for improving electroanalytical selectivity: application to selective dopamine detection in the presence of ascorbic acid. *ChemPhysChem*. 2013;14:1887–98. doi:10.1002/cphc.201300134.
- Valentini F, Ciambella E, Conte V, Sabatini L, Ditaranto N, Cataldo F, et al. Highly selective detection of epinephrine at oxidized single-wall carbon nanohorns modified screen printed electrodes (SPEs). *Biosens Bioelectron*. 2014;59:94–8. doi:10.1016/j.bios.2014.02.065.
- Tan SM, Poh HL, Sofer Z, Pumera M. Boron-doped graphene and boron-doped diamond electrodes: detection of biomarkers and resistance to fouling. *Analyst*. 2013;138:4885–91. doi:10.1039/c3an00535f.
- Silvestrini M, Schiavuta P, Scopece P, Pecchiola G, Moretto LM, Ugo P. Modification of nanoelectrode ensembles by thiols and disulfides to prevent non specific adsorption of proteins. *Electrochim Acta*. 2011;56:7718–24. doi:10.1016/j.electacta.2011.06.034.
- Sanghavi BJ, Wolfbeis OS, Hirsch T, Swami NS. Nanomaterial-based electrochemical sensing of neurological drugs and neurotransmitters. *Microchim Acta*. 2014;182:1–41. doi:10.1007/s00604-014-1308-4.
- Jackowska K, Kryszynski P. New trends in the electrochemical sensing of dopamine. *Anal Bioanal Chem*. 2013;405:3753–71. doi:10.1007/s00216-012-6578-2.
- Olsson J, Winquist F, Lundström I. A self polishing electronic tongue. *Sensors Actuators B Chem*. 2006;118:461–5. doi:10.1016/j.snb.2006.04.042.
- Özcan A, Şahin Y. Selective and sensitive voltammetric determination of dopamine in blood by electrochemically treated pencil graphite electrodes. *Electroanalysis*. 2009;21:2363–70. doi:10.1002/elan.200904695.
- Soliveri G, Pifferi V, Panzarasa G, Ardizzone S, Cappelletti G, Meroni D, et al. Self-cleaning properties in engineered sensors for dopamine electroanalytical detection. *Analyst*. 2015;140:1486–94. doi:10.1039/c4an02219j.
- Pifferi V, Soliveri G, Panzarasa G, Ardizzone S, Cappelletti G, Meroni D, et al. Electrochemical sensors cleaned by light: a proof of concept for on site applications towards integrated monitoring systems. *RSC Adv*. 2015;5:71210–4. doi:10.1039/C5RA12219H.
- Wang X, Xiong R, Wei G. Preparation of mesoporous silica thin films on polystyrene substrate by electrochemically induced sol-gel technique. *Surf Coat Technol*. 2010;204:2187–92. doi:10.1016/j.surfcoat.2009.12.003.
- Maino G, Meroni D, Pifferi V, Falcicola L, Soliveri G, Cappelletti G, et al. Electrochemically assisted deposition of transparent, mechanically robust TiO₂ films for advanced applications. *J Nanoparticle Res*. 2013;15:2087. doi:10.1007/s11051-013-2087-2.
- Antonello A, Soliveri G, Meroni D, Cappelletti G, Ardizzone S. Photocatalytic remediation of indoor pollution by transparent TiO₂ films. *Catal Today*. 2014;230:35–40. doi:10.1016/j.cattod.2013.12.033.

28. Panzarasa G. Shining light on nanochemistry using silver nanoparticle-enhanced luminol chemiluminescence. *J Chem Educ.* 2014;91:696–700. doi:10.1021/ed400736k.
29. Pifferi V, Facchinetti G, Villa A, Prati L, Falciola L. Electrocatalytic activity of multiwalled carbon nanotubes decorated by silver nanoparticles for the detection of halothane. *Catal Today.* 2014. doi:10.1016/j.cattod.2014.10.006.
30. Falciola L, Gennaro A, Isse AA, Mussini PR, Rossi M. The solvent effect in the electrocatalytic reduction of organic bromides on silver. *J Electroanal Chem.* 2006;593:47–56. doi:10.1016/j.jelechem.2006.02.003.
31. Bellomunno C, Bonanomi D, Falciola L, Longhi M, Mussini PR, Doubova LM, et al. Building up an electrocatalytic activity scale of cathode materials for organic halide reductions. *Electrochim Acta.* 2005;50:2331–41. doi:10.1016/j.electacta.2004.10.047.
32. Pifferi V, Marona V, Longhi M, Falciola L. Characterization of polymer stabilized silver nanoparticles modified glassy carbon electrodes for electroanalytical applications. *Electrochim Acta.* 2013;109:447–53. doi:10.1016/j.electacta.2013.07.194.
33. Welch CM, Compton RG. The use of nanoparticles in electroanalysis: a review. *Anal Bioanal Chem.* 2006;384:601–19. doi:10.1007/s00216-005-0230-3.
34. Campbell FW, Compton RG. The use of nanoparticles in electroanalysis: an updated review. *Anal Bioanal Chem.* 2010;396:241–59. doi:10.1007/s00216-009-3063-7.
35. Herzog G, Beni V. Stripping voltammetry at micro-interface arrays: a review. *Anal Chim Acta.* 2013;769:10–21. doi:10.1016/j.aca.2012.12.031.
36. Simm AO, Ward-Jones S, Banks CE, Compton RG. Novel methods for the production of silver microelectrode-arrays: their characterisation by atomic force microscopy and application to the electroreduction of halothane. *Anal Sci.* 2005;21:667–71. doi:10.2116/analsci.21.667.
37. Daniele S, Baldo M, Bragato C. Recent developments in stripping analysis on microelectrodes. *Curr Anal Chem.* 2008;4:215–28. doi:10.2174/157341108784911343.
38. Syres K, Thomas A, Bondino F, Malvestuto M, Grätzel M. Dopamine adsorption on anatase TiO₂(101): a photoemission and NEXAFS spectroscopy study. *Langmuir.* 2010;26:14548–55. doi:10.1021/la1016092.
39. Jackman MJ, Syres KL, Cant DJH, Hardman SJO, Thomas AG. Adsorption of dopamine on rutile TiO₂ (110): a photoemission and near-edge X-ray absorption fine structure study. *Langmuir.* 2014;30:8761–9. doi:10.1021/la501357b.
40. Song P, Guo X, Pan Y, Wen Y, Zhang Z, Yang H. SERS and in situ SERS spectroelectrochemical investigations of serotonin monolayers at a silver electrode. *J Electroanal Chem.* 2013;688:384–91. doi:10.1016/j.jelechem.2012.09.008.
41. Currie LA. Nomenclature in evaluation of analytical methods including detection and quantification capabilities (IUPAC Recommendations 1995). *Pure Appl Chem.* 1995;67:1699–723. doi:10.1351/pac199567101699.
42. Thompson M, Ellison SLR, Wood R. Harmonized guidelines for single-laboratory validation of methods of analysis (IUPAC Technical Report). *Pure Appl Chem.* 2002;74:835–55. doi:10.1351/pac200274050835.
43. Yin T, Wei W, Zeng J. Selective detection of dopamine in the presence of ascorbic acid by use of glassy-carbon electrodes modified with both polyaniline film and multi-walled carbon nanotubes with incorporated beta-cyclodextrin. *Anal Bioanal Chem.* 2006;386:2087–94. doi:10.1007/s00216-006-0845-z.
44. Hanly G, Fornasiero D, Ralston J, Sedev R. Electrostatics and metal oxide wettability. *J Phys Chem C.* 2011;115:14914–21. doi:10.1021/jp203714a.
45. Koktysh DS, Liang X, Yun B-G, Pastoriza-Santos I, Matts RL, Giersig M, et al. Biomaterials by design: layer-by-layer assembled ion-selective and biocompatible films of TiO₂ nanoshells for neurochemical monitoring. *Adv Funct Mater.* 2002;12:255. doi:10.1002/1616-3028(20020418)12:4<255::AID-ADFM255>3.0.CO;2-1.
46. McNay EC, Sherwin RS. From artificial cerebro-spinal fluid (aCSF) to artificial extracellular fluid (aECF): microdialysis perfusate composition effects on in vivo brain ECF glucose measurements. *J Neurosci Methods.* 2004;132:35–43. doi:10.1016/j.jneumeth.2003.08.014.
47. Shiobara R, Ohira T, Doi K, Nishimura M, Kawase T. Development of artificial cerebrospinal fluid: basic experiments, and phase II and III clinical trials. *J Neurol Neurophysiol.* 2013. doi:10.4172/2155-9562.1000173.
48. Wang Z, Wu J, Wu S, Bao A. High-performance liquid chromatographic determination of histamine in biological samples: the cerebrospinal fluid challenge—a review. *Anal Chim Acta.* 2013;774:1–10. doi:10.1016/j.aca.2012.12.041.
49. Fang L, Lv Y, Sheng X, Yao S. Sensitive, rapid and easy analysis of three catecholamine metabolites in human urine and serum by liquid chromatography tandem mass spectrometry. *J Chromatogr Sci.* 2012;50:450–6. doi:10.1093/chromsci/bms068.
50. Meintjes M, Chantilis SJ, Ward DC, Douglas JD, Rodriguez AJ, Guerami AR, et al. A randomized controlled study of human serum albumin and serum substitute supplement as protein supplements for IVF culture and the effect on live birth rates. *Hum Reprod.* 2009;24:782–9. doi:10.1093/humrep/den396.
51. Rauch C, Feifel E, Amann E-M, Spötl HP, Schennach H, Pfaller W, et al. Alternatives to the use of fetal bovine serum: human platelet lysates as a serum substitute in cell culture media. *ALTEX.* 2011;28:305–16.